

1  
2  
3  
4  
5  
6  
7  
8  
9  
10  
11  
12  
13  
14  
15  
16  
17  
18  
19  
20  
21  
22  
23  
24  
25  
26  
27  
28  
29

**Optical properties and bioavailability of dissolved organic matter along a flow-path continuum from soil pore waters to the Kolyma River mainstem, East Siberia**

Karen E. Frey<sup>1,\*</sup>, William V. Sobczak<sup>2</sup>, Paul J. Mann<sup>3</sup>, R. Max Holmes<sup>4</sup>

<sup>1</sup>*Graduate School of Geography, Clark University, Worcester, Massachusetts 01610 USA*

<sup>2</sup>*Department of Biology, College of the Holy Cross, Worcester, Massachusetts 01610 USA*

<sup>3</sup>*Department of Geography, Northumbria University, Newcastle upon Tyne NE1 8ST UK*

<sup>4</sup>*Woods Hole Research Center, Falmouth, Massachusetts 02540 USA*

\*Corresponding author: [kfrey@clarku.edu](mailto:kfrey@clarku.edu); Tel: 1.508.793.7209

**Keywords:** East Siberia, Kolyma River, permafrost, DOC, CDOM, biolability

30 **Abstract**

31 The Kolyma River in Northeast Siberia is among the six largest arctic rivers and drains a region  
32 underlain by vast deposits of Holocene-aged peat and Pleistocene-aged loess known as yedoma,  
33 most of which is currently stored in ice-rich permafrost throughout the region. These peat and  
34 yedoma deposits are important sources of dissolved organic matter (DOM) to inland waters that  
35 in turn play a significant role in the transport and ultimate remineralization of organic carbon to  
36 CO<sub>2</sub> and CH<sub>4</sub> along the terrestrial flow-path continuum. The turnover and fate of terrigenous  
37 DOM during offshore transport largely depends upon the composition and amount of carbon  
38 released to inland and coastal waters. Here, we measured the ultraviolet-visible optical  
39 properties of chromophoric DOM (CDOM) from a geographically extensive collection of waters  
40 spanning soil pore waters, streams, rivers, and the Kolyma River mainstem throughout a ~250  
41 km transect of the northern Kolyma River basin. During the period of study, CDOM absorption  
42 coefficients were found to be robust proxies for the concentration of DOM, whereas additional  
43 CDOM parameters such as spectral slopes (*S*) were found to be useful indicators of DOM quality  
44 along the flow-path. In particular, the spectral slope ratio (*S<sub>R</sub>*) of CDOM demonstrated  
45 statistically significant differences between all four water types and tracked changes in the  
46 concentration of bioavailable DOC, suggesting that this parameter may be suitable for clearly  
47 discriminating shifts in organic matter characteristics among water types along the full flow-path  
48 continuum across this landscape. However, despite our observations of downstream shifts in  
49 DOM composition, we found a relatively constant proportion of DOC that was bioavailable (~3–  
50 6% of total DOC) regardless of relative water residence time along the flow-path. This may be a  
51 consequence of two potential scenarios allowing for continual processing of organic material  
52 within the system, namely: (a) aquatic microorganisms are acclimating to a downstream shift in

53 DOM composition; and/or (b) photodegradation is continually generating labile DOM for  
54 continued microbial processing of DOM along the flow-path continuum. Without such  
55 processes, we would otherwise expect to see a declining fraction of bioavailable DOC  
56 downstream with increasing residence time of water in the system. With ongoing and future  
57 permafrost degradation, peat and yedoma deposits throughout the Northeast Siberian region will  
58 become more hydrologically active, providing greater amounts of DOM to fluvial networks and  
59 ultimately to the Arctic Ocean. The ability to rapidly and comprehensively monitor shifts in the  
60 quantity and quality of DOM across the landscape is therefore critical for understanding potential  
61 future feedbacks within the arctic carbon cycle.

62

## 63 **1. Introduction**

64       There is increasing evidence that inland freshwater ecosystems play a significant role in  
65 the global carbon cycle owing to the metabolism of terrestrially-derived organic matter as it  
66 moves through fluvial networks from land to ocean (Cole et al., 2007; Battin et al., 2009a, b).  
67 Recent research suggests that arctic watersheds may increasingly augment the role of freshwater  
68 ecosystems in the global flux of terrestrial carbon to the atmosphere (Walter et al., 2007; Denfeld  
69 et al., 2013; Vonk et al., 2013; Hayes et al., 2014; Spencer et al., 2015) and ocean (Frey and  
70 Smith, 2005; Frey and McClelland, 2009; Schreiner et al., 2014; Tesi et al., 2014) as a result of  
71 climate warming and changing regional hydrology. Terrestrial sources of organic matter  
72 generally dominate the energy and carbon fluxes through stream, riverine, and estuarine  
73 ecosystems (Mulholland, 1997; Holmes et al., 2008), but the lability and composition of this  
74 carbon remain poorly characterized. Headwater and intermediate streams dominate overall  
75 channel length in large dendritic drainage basins (e.g., Denfeld et al., 2013), thus the functional

76 role of streams and intermediate rivers is magnified when assessing landscape controls on carbon  
77 and nutrient fluxes to the atmosphere and Arctic Ocean.

78         Following the publication of the “river continuum concept” (Vannote et al., 1980), there  
79 has been much research focused on the delivery and processing of terrestrially-derived organic  
80 matter within temperate stream ecosystems. Through these studies, it has been shown that  
81 biological processes within streams alter the transport of organic matter to downstream  
82 ecosystems (e.g., Webster and Meyer, 1997), but the fate of terrestrial organic matter in arctic  
83 streams and rivers has only more recently been explored (e.g., Frey and Smith, 2005; Neff et al.,  
84 2006; Holmes et al., 2008; Denfeld et al., 2013; Spencer et al., 2015). Furthermore, a variety of  
85 conceptual and pragmatic issues complicate the study of arctic rivers, including: (i) large  
86 seasonal variations in discharge accompanied by large seasonal variations in nutrient and organic  
87 matter inputs from rivers to the coastal ocean (e.g., McClelland et al., 2012); (ii) the  
88 heterogeneity of vegetation, permafrost extent, topography, and soil attributes within arctic  
89 watersheds (e.g., Frey and McClelland, 2009); and (iii) spatial and temporal inaccessibility  
90 hindering comprehensive sampling; among others.

91         Hydrologic flow-paths and organic matter transport in arctic regions dominated by  
92 permafrost are markedly different than temperate regions with well-drained soils. In particular,  
93 permafrost-dominated watersheds lack deep groundwater flow-paths owing to the permafrost  
94 boundary in soil that prevents deep groundwater movement (Judd and Kling, 2002; Frey et al.,  
95 2007). As a result, the delivery of terrestrial-permafrost organic matter to aquatic ecosystems  
96 may in fact lack significant terrestrial or groundwater processing. Once dissolved organic matter  
97 (DOM) enters aquatic ecosystems, multiple processes remove DOM from the water column: (i)  
98 photochemical reactions, where DOM is degraded to CO<sub>2</sub> or to compounds bioavailable for

99 bacterial uptake (Moran and Zepp, 1997; Laurion and Mladenov, 2013; Cory et al., 2014); (ii)  
100 loss via aggregation of DOM owing to changes in ionic strength when freshwater mixes with sea  
101 water (Sholkovitz, 1976); (iii) DOM sorption to particles and sedimentation (Chin et al., 1998);  
102 and/or (iv) bacterial uptake and utilization of the bioavailable fraction (Bronk, 2002; Karl and  
103 Björkman, 2002; Mann et al., 2014; Spencer et al., 2015). Measurements of waters along a  
104 hydrologic flow-path may indeed give insight into the characteristics of DOM as it is modified  
105 through these various processes along the soil-stream-river continuum.

106         Recent work on the Kolyma River in Northeast Siberia has identified marked variation in  
107 annual discharge that is associated with large pulses of organic matter flux to the Arctic Ocean  
108 during spring freshet, providing detailed temporal characterization of DOM in the Kolyma River  
109 mainstem across the annual hydrograph (e.g., Mann et al., 2012). Furthermore, selective  
110 processing and loss of permafrost-derived DOM has been shown to occur via microbial  
111 metabolism throughout the Kolyma River basin, as waters move downstream through the fluvial  
112 network (Mann et al., 2014; Mann et al., 2015; Spencer et al., 2015). Here, we complement  
113 these previous studies by providing extensive spatial characterization of DOM along a flow-path  
114 continuum from soil pore waters to the Kolyma River mainstem during mid-summer (July)  
115 baseflow. The heterogeneity of environmental characteristics and extensive continuous  
116 permafrost of the Kolyma River basin combine to make this a critical region to investigate and  
117 monitor. In particular, we measured the ultraviolet-visible absorption spectra (200–800 nm) of  
118 chromophoric DOM (CDOM) from a geographically extensive collection of waters throughout a  
119 ~250 km transect of the northern Kolyma River basin, including samples of soil pore waters,  
120 streams, rivers, and the Kolyma River mainstem. CDOM absorption and spectral slopes  
121 (calculated within log-transformed absorption spectra) were used to investigate contrasting water

122 types and were found to be useful indicators of both the concentration and reactivity of DOM.  
123 With ongoing permafrost degradation and subsequent release of a long-term storehouse of  
124 organic material into the contemporary carbon cycle, the ability to easily and comprehensively  
125 monitor the quantity and quality of DOM across the landscape through investigation of its optical  
126 properties is becoming critical for understanding the global significance of the arctic carbon  
127 cycle. Here, we explore a full suite of CDOM parameters as well as concentrations of dissolved  
128 organic carbon (DOC) and bioavailable DOC as they vary across a full flow-path continuum in  
129 the Kolyma River basin in Northeast Siberia.

130

## 131 **2. Data and Methods**

132 The Kolyma River in Northeast Siberia is among the six largest arctic rivers and drains a  
133 ~650,000 km<sup>2</sup> region underlain by vast deposits of Holocene-aged peat and Pleistocene-aged  
134 loess known as yedoma, much of which is currently stored in ice-rich permafrost throughout the  
135 region (Holmes et al., 2012; Holmes et al., 2013). These peats and yedoma deposits are  
136 important sources of DOM to terrestrial waters that in turn play a significant role in the transport  
137 and ultimate remineralization of organic carbon to atmospheric CO<sub>2</sub> and CH<sub>4</sub> (e.g., Walter et al.,  
138 2006; Mann et al., 2012; Denfeld et al., 2013; Spencer et al., 2015). The Kolyma River basin  
139 and its subwatersheds exhibit extreme hydrologic seasonality, with ice breakup and peak river  
140 discharge typically occurring in late May or early June. In this study, sampling took place along  
141 the most northern ~250 km of the Kolyma River in the vicinity of Cherskiy, Sakha Republic,  
142 Russia (68.767°N, 161.333°E) during the mid-summer period of July 2009 (Figure 1). Samples  
143 were collected over a narrow temporal window from July 11–25, 2009 in order to capture a  
144 “snapshot” of observations during the mid-summer period. In total, 47 water samples were

145 collected, including soil pore waters in shallow wetlands (n=9), small streams with watersheds  
146 <100 km<sup>2</sup> (n=15), major river tributaries with watersheds 900–120,000 km<sup>2</sup> (n=14), and Kolyma  
147 mainstem locations with watersheds >400,000 km<sup>2</sup> (n=9). Although we did not determine  
148 residence times directly for our sampled sites, Vonk et al. (2013) estimated that in higher relief  
149 areas near Duvannyi Yar (adjacent to the Kolyma River mainstem), the transport time from  
150 permafrost thaw to entry into the Kolyma River may be less than one hour. Furthermore, with  
151 respect to the mainstem, it has been estimated that water residence times in the Kolyma River  
152 from Duvannyi Yar to the river mouth may be ~3–7 days, assuming average mainstem velocities  
153 of 0.5–1.5 m/s (Holmes et al., 2012; Vonk et al., 2013). As such, permafrost-derived C may not  
154 be easily detectable at the river mouth, as this time is likely comparable to the rapid removal  
155 rates of highly labile permafrost C determined through incubation experiments (e.g., Holmes et  
156 al., 2012; Vonk et al., 2013).

157         Samples were collected by hand using a 1 L acid-washed high density polyethylene  
158 (HDPE) bottle as a collection vessel, where sample waters were used to rinse the bottle several  
159 times before filling. Soil pore waters were collected by depressing the soil surface within the  
160 wetlands and allowing the water to slowly seep into the collection vessel. In shallow streams,  
161 less than 0.5 m in depth, samples were collected approximately midway below the surface and  
162 the bottom. In larger tributaries and rivers, samples were collected at a depth of ~0.5 m. Water  
163 samples were then filtered through precombusted (450°C for 6 hours) Whatman 0.7 µm GF/F  
164 filters in the field and stored in acid-washed HDPE bottles without headspace to minimize  
165 degassing and algal growth. Upon returning to the laboratory (typically within ~1 day), DOC  
166 samples were acidified with concentrated HCl to a pH of ≤2 and stored refrigerated and in the  
167 dark until analysis via high-temperature combustion using a Shimadzu TOC-VCPH Analyzer

168 (within one month of collection). DOC was calculated as the mean of 3 to 5 injections with a  
169 coefficient of variance less than 2%.

170 We additionally conducted a series of organic matter bioavailability assays to assess the  
171 total and relative amounts of bioavailable DOC in soil, stream, and river environments. These  
172 assays relied upon 5-day biological oxygen demand (BOD) incubations, with methods similar to  
173 those in Mann et al. (2014). Water samples were collected in triplicate glass 300 mL BOD  
174 bottles and filtered as DOC (above). The samples were initially allowed to equilibrate via  
175 filtering in a controlled laboratory environment at 15°C, after which t=0 was the start time of the  
176 incubations. The Winkler titration method was used to measure dissolved oxygen (DO)  
177 concentrations initially (t=0) (i.e., in situ DO) as well as after 5-day incubations at 15°C, where  
178 bottles were kept in the dark in between measurements. At t=0, DO measurements were at  
179 concentrations expected at equilibrium with the 15°C laboratory temperature (~8.5–9.0 mg/L).  
180 This temperature was only slightly warmer than environmental sampling conditions (i.e., the  
181 Kolyma River mainstem samples ranged from 11.40–13.90°C, river samples ranged from 10.70–  
182 14.20°C, and stream samples ranged from 4.40–13.80°C). However, we maintained samples at  
183 15°C as is standard in the BOD method, which allowed samples to be treated identically in the  
184 controlled experiment (in situ temperatures varied depending not only upon location but also  
185 date and time of day). Furthermore, bottles were wrapped tightly with paraffin such that  
186 physical degassing should have been minimal during the incubations. BOD was then calculated  
187 as the difference between DO concentrations at t = 0 and following the 5-day incubations. We  
188 assumed 100% of DO consumed was converted to CO<sub>2</sub> via aerobic respiration and that the  
189 carbon source respired was DOM, where resulting BOD measurements were used an analog for  
190 bioavailable DOC. The Winkler method we used here has been used extensively and is attractive



191 for a variety of reasons, including: (i) enabling DO to be measured with precision of 0.01 mg/L,  
192 thus low respiration rates can be accurately measured; (ii) allowing for convenient replication of  
193 assays within habitats; (iii) permitting experimental manipulation of standard bioassays (e.g., N  
194 and P amendments, photolysis experiments, alteration of initial microbial consortia, and  
195 temperature manipulation; (iv) helping to segregate the relative roles of water column and  
196 sediment processes (through comparisons with sediment analyses); and (v) helping to inform  
197 more realistic ecosystem-level experiments that are much more laborious and time intensive.

198 In order to investigate the optical characteristics of the DOM in these samples, we  
199 additionally measured the ultraviolet-visible absorption spectra of CDOM from this broad  
200 collection of waters. CDOM absorbance was measured on filtered (precombusted Whatman 0.7  
201  $\mu\text{m}$  GF/F), unacidified waters stored in acid-washed HDPE bottles immediately after collection  
202 (within  $\sim 1$  day) at the Northeast Science Station in Cherskiy using a Thermo Scientific  
203 GENESYS 10 UV/Vis Spectrophotometer across wavelengths 800–200 nm (1 nm interval) with  
204 a 1 cm quartz cuvette. All sample spectra were blank corrected using Milli-Q water (18  $\Omega$ ).  
205 Measurements were made after samples had equilibrated to the laboratory temperature in order  
206 to minimize temperature effects. Null-point adjustments were performed on all spectra, such that  
207 CDOM absorbance was assumed to be zero across wavelengths greater than 750 nm and the  
208 average absorbance between 750 nm and 800 nm was subtracted from each spectrum to correct  
209 for offsets owing to instrument baseline drift, temperature, scattering, and refractive effects  
210 (Green and Blough, 1994; Helms et al, 2008). CDOM absorption coefficients were calculated  
211 as:

212 
$$a(\lambda) = 2.303A(\lambda)/l \quad (1)$$

213 where  $a$  is the Napierian absorption coefficient ( $\text{m}^{-1}$ ) at a specified wavelength ( $\lambda$ , in nm),  $A(\lambda)$  is  
214 the absorbance at the wavelength, and  $l$  is the cell path length in meters (Green and Blough,  
215 1994). To avoid inner-filtering effects, several highly absorbing samples (primarily the soil pore  
216 waters) were diluted with Milli-Q water before analysis (to the point where  $A_{350}$  at a 1 cm path  
217 length was  $\leq 0.02$ ) to avoid saturation of the spectra at short wavelengths, where the final CDOM  
218 absorbance and therefore absorption coefficients were corrected for these procedures.

219 CDOM spectral slopes ( $S$ ,  $\text{nm}^{-1}$ ) between 290–350 nm ( $S_{290-350}$ ), 275–295 nm ( $S_{275-295}$ ),  
220 and 350–400 nm ( $S_{350-400}$ ), calculated within log-transformed absorption spectra, were also  
221 utilized to investigate DOM characteristics of contrasting water types, and were calculated as:

$$222 \quad a(\lambda) = a(\lambda_{ref}) e^{-S(\lambda - \lambda_{ref})} \quad (2)$$

223 where  $a(\lambda)$  is the absorption coefficient at a specified wavelength,  $\lambda_{ref}$  is a reference wavelength,  
224 and  $S$  is the slope fitting parameter (Hernes et al., 2008; Helms et al., 2008; Spencer et al.,  
225 2009a). All slopes are reported here as positive values, such that higher (i.e., steeper) slopes  
226 indicate a greater decrease in absorption with increasing wavelength. Additional CDOM  
227 parameters investigated here include the spectral slope ratio ( $S_R$ ), calculated as the ratio between  
228  $S_{275-295}$  and  $S_{350-400}$ ; the ratio between CDOM absorption coefficients ( $a$ ) at 250 nm and 365 nm  
229 ( $a_{250}:a_{365}$ ); and specific UV absorbance ( $\text{SUVA}_{254}$ ), determined by dividing UV absorbance ( $A$ )  
230 at 254 nm by the sample DOC concentration and reported in units of  $\text{L mg C}^{-1} \text{ m}^{-1}$  (Weishaar et  
231 al., 2003). These six CDOM parameters ( $S_{290-350}$ ,  $S_{275-295}$ ,  $S_{350-400}$ ,  $a_{250}:a_{365}$ ,  $\text{SUVA}_{254}$ , and  $S_R$ )  
232 have been shown to provide insights for various DOM characteristics such as molecular weight,  
233 source waters, composition, age, and aromatic content for a variety of geographic regions (e.g.,  
234 Weishaar 2003; Neff et al., 2006; Helms et al., 2008; Spencer et al., 2008; Spencer et al., 2009a;  
235 Spencer et al., 2009b; Mann et al., 2012). As such, we chose our method for spectral slope

236 calculations to be consistent with previous studies to foster intercomparisons between datasets,  
237 however future studies may derive further insight utilizing methods that calculate a continuous  
238 spectral slope curve over the full 200–800 nm span (e.g., Loiselle et al., 2009) rather than only  
239 specific wavelength intervals as presented here.

240

### 241 **3. Results**

242 Total DOC concentrations (and the variance among values within each water type)  
243 decreased markedly downstream along the flow-path continuum from soil pore waters to the  
244 Kolyma River mainstem (Figure 2a). Mean ( $\pm 1$  standard deviation) DOC values were  $43.3 \pm$   
245  $22.8 \text{ mg L}^{-1}$  (soil pore waters),  $11.6 \pm 3.0 \text{ mg L}^{-1}$  (streams),  $4.9 \pm 1.6 \text{ mg L}^{-1}$  (rivers), and  $3.6 \pm$   
246  $0.4 \text{ mg L}^{-1}$  (mainstem waters). Soil pore waters, in particular, showed highly variable DOC  
247 concentrations (ranging from 13.2 to  $64.7 \text{ mg L}^{-1}$ ) demonstrating the heterogeneous supply of  
248 DOM from terrestrial systems to streams. By contrast, DOC concentrations in the Kolyma  
249 mainstem along the ~250 km stretch sampled were remarkably similar (ranging from 3.0 to 4.4  
250  $\text{mg L}^{-1}$ ) during this mid-summer July period (Figure 2a). Furthermore, DOC concentrations of  
251 the four water types sampled were found to be significantly different from one another (one-way  
252 ANOVA,  $p < 0.05$ ).

253 Concentrations of bioavailable DOC showed similar patterns to DOC, declining  
254 downstream along the flow-path continuum with increasing water residence time in the system  
255 (Figure 2b). Bioavailable DOC concentrations averaged  $0.9 \pm 0.2 \text{ mg L}^{-1}$  (soil pore waters),  $0.3$   
256  $\pm 0.1 \text{ mg L}^{-1}$  (streams),  $0.3 \pm 0.2 \text{ mg L}^{-1}$  (rivers), and  $0.2 \pm 0.2 \text{ mg L}^{-1}$  (mainstem waters), and  
257 showed relative greater variability than DOC within the stream, river and mainstem water types.  
258 Concentrations of bioavailable DOC in soil pore waters were statistically different from the other

259 three water types (one-way ANOVA,  $p < 0.05$ ), although by contrast, streams, rivers, and  
260 mainstem waters were not statistically different from one another ( $p > 0.05$ ). Importantly, the  
261 percentage of bioavailable DOC (i.e., calculated as the amount of bioavailable DOC divided by  
262 total DOC) did not significantly decrease downstream (one-way ANOVA,  $p > 0.05$ ) and showed  
263 relatively similar values among the four water sample types along the flow-path continuum  
264 (Figure 2c), where percentages averaged  $3.9 \pm 3.8\%$  (soil pore waters),  $3.2 \pm 1.9\%$  (streams),  $6.2$   
265  $\pm 4.3\%$  (rivers), and  $4.5 \pm 4.5\%$  (mainstem waters).

266 CDOM absorption spectra (200–800 nm) showed clear separation between soil pore  
267 waters, streams, rivers, and the Kolyma mainstem, where soil pore waters exhibited values  
268 markedly higher than the other three water sample types (Figure 3a). CDOM absorption also  
269 clearly declined downstream from streams, rivers, to mainstem waters when assessing those  
270 waters only (Figure 3b). Furthermore, we investigated the potential for utilizing CDOM  
271 absorption as a proxy for DOC concentrations in these waters. Our data revealed that  
272 independent of water type along the stream-river-mainstem flow-path, CDOM absorption was  
273 strongly linearly correlated to DOC concentrations at 254, 350, and 440 nm (Figure 4). In  
274 particular, CDOM absorption at 254 nm had the highest predictive capability of DOC ( $r^2 =$   
275  $0.958$ ,  $p < 0.01$ ), with CDOM absorption at 350 nm ( $r^2 = 0.855$ ,  $p < 0.01$ ) and 440 nm ( $r^2 = 0.667$ ,  
276  $p < 0.01$ ) less strongly predictive (Figure 4).

277 We additionally investigated the quantitative distribution of the six derived CDOM  
278 parameters ( $S_{290-350}$ ,  $S_{275-295}$ ,  $S_{350-400}$ ,  $a_{250}:a_{365}$ ,  $SUVA_{254}$ , and  $S_R$ ) across the four water types  
279 (Figure 5; Table 1). In general, four parameters ( $S_{290-350}$ ,  $S_{275-295}$ ,  $a_{250}:a_{365}$ , and  $S_R$ ) showed an  
280 increasing pattern along the flow-path continuum, whereas two parameters ( $S_{350-400}$  and  
281  $SUVA_{254}$ ) showed a decreasing pattern. In terms of whether the values of the six parameters

282 were statistically significantly different among water sample types, one-way ANOVA tests (at  
283 the 0.05 level) revealed inconsistent results. Most commonly, soil pore waters were statistically  
284 different from all other water types for four of the parameters ( $S_{290-350}$ ,  $S_{275-295}$ ,  $a_{250}:a_{365}$ , and  $S_R$ ),  
285 but no consistent pattern was observed in significant differences across other water types.  
286 However, the spectral slope ratio ( $S_R$ ) was the only CDOM parameter of the six investigated that  
287 showed statistically significant differences between all four water types ( $p < 0.05$ ).

288         Lastly, we examined the relationships between CDOM optical properties and DOM  
289 bioavailability. To this end, we performed linear regressions between all six of our derived  
290 CDOM parameters and bioavailable DOC concentrations to determine the strength of their  
291 ability to predict bioavailable DOC. Our results indicated that five of the CDOM parameters  
292 ( $S_{290-350}$ ,  $S_{275-295}$ ,  $a_{250}:a_{365}$ ,  $SUVA_{254}$ , and  $S_R$ ) were statistically significant predictors at the 0.05  
293 level (Table 2). In particular,  $S_R$  showed the strongest relationship with bioavailable DOC  
294 concentrations ( $r^2$  value = 0.45,  $p < 0.01$ ). The relationship between bioavailable DOC  
295 concentrations and  $S_R$  (Figure 6) showed a distinct negative trend (bioavailable DOC  $\text{mg L}^{-1} = -$   
296  $2.204(S_R) + 2.518$ ), with the highest bioavailable DOC concentrations and lowest  $S_R$  values for  
297 soil pore waters, and lowest bioavailable DOC concentrations and highest  $S_R$  values for Kolyma  
298 River mainstem waters. We found a clear gradation in the relationship between  $S_R$  and  
299 bioavailable DOC down the flow-path continuum, as one would also expect by examining these  
300 parameters individually (e.g., Figures 2b, 5f). In summary, not only was  $S_R$  the only CDOM  
301 parameter that showed statistically significant separation between all four water types examined,  
302 but it also had the strongest relationship when compared with concentrations of bioavailable  
303 DOC.

304

#### 305 **4. Discussion and Conclusions**

306 In this study, we present a full suite of DOC, bioavailable DOC, and CDOM parameters  
307 throughout the permafrost-dominated Kolyma River basin in Northeast Siberia with the purpose  
308 of helping to elucidate the processing of DOM along a full flow-path continuum from soil pore  
309 waters to the mainstem. Our findings show that average concentrations of DOC and bioavailable  
310 DOC generally decrease as waters travel downstream from soil pore waters, streams, rivers, and  
311 ultimately to the Kolyma River mainstem. This pattern suggests the occurrence of rapid in-  
312 stream processing of DOM and potential remineralization of DOC to atmospheric CO<sub>2</sub> during  
313 this July baseflow period well before these waters reach the Arctic Ocean (e.g., Denfeld et al.,  
314 2013; Mann et al., 2015; Spencer et al., 2015). The amount of total DOC putatively lost to  
315 remineralization is a relatively small fraction (~3–6% depending upon water type), but on par  
316 with similar studies across the Arctic for this time of year (e.g., Holmes et al., 2008). Although  
317 this may be a relatively small proportion, it is likely the permafrost-derived, ancient DOC found  
318 in headwaters that is contributing to permafrost carbon feedbacks to climate warming (Mann et  
319 al., 2015). Moving downstream, the river continuum concept predicts that relative diversity of  
320 organic molecules decreases from the headwaters to the river mouth (Vannote et al., 1980). As  
321 energetically favorable compounds are converted to living tissue or respired as CO<sub>2</sub>, bulk DOM  
322 in the Kolyma basin has indeed been shown in previous studies to become less diverse moving  
323 from headwaters to mainstem waters before exported to the Arctic Ocean (Spencer et al., 2015).

324 CDOM parameters presented in this study give further insight into characteristics of  
325 DOM along the full flow-path continuum throughout the Kolyma River basin. For instance, the  
326 specific ultraviolet absorbance (SUVA<sub>254</sub>) has been shown to be correlated with DOM  
327 composition, where SUVA<sub>254</sub> values are positively correlated with percent aromaticity and

328 molecular size of DOM (and for a given river have been shown to be greatest during spring  
329 flood) (e.g., Weishaar et al., 2003; Spencer et al., 2009a; Mann et al., 2012). In this study, we  
330 generally found progressively decreasing  $SUVA_{254}$  values along the flow-path from soil pore  
331 waters towards mainstem waters, suggesting that soil pore waters contain higher molecular  
332 weight, aromatic terrestrial DOM that generally becomes lower in molecular weight and  
333 aromaticity along the flow-path continuum towards the Kolyma River mainstem. In addition, the  
334  $a_{250}:a_{365}$  ratio has been shown to be negatively correlated to aromaticity and molecular size of  
335 DOM (Peuravuori and Pihlaja, 1997). In fact (similar to samples from the Yukon River, Alaska  
336 (Spencer et al., 2009a)), our data showed that the  $a_{250}:a_{365}$  ratio is significantly negatively  
337 correlated with  $SUVA_{254}$  ( $a_{250}:a_{365} = -0.947 (SUVA_{254}) - 0.947; r^2=0.49, p<0.01$ ). As such, the  
338  $a_{250}:a_{365}$  ratio may potentially be utilized as a first-order proxy for  $SUVA_{254}$  when DOC  
339 concentrations cannot be easily determined.

340         However, despite our observations of downstream shifts in DOM composition, we find a  
341 relatively constant proportion of DOC that was bioavailable (~3–6% of total DOC) regardless of  
342 relative water residence time along the flow-path. This suggests that continual microbial  
343 processing of organic matter is able to occur with similar rates during transit from headwaters  
344 throughout the Kolyma River drainage network to the Arctic Ocean concurrent with ongoing  
345 downstream CDOM compositional changes. Microbial demand in headwater streams of the  
346 Kolyma River basin is subsidized by significant quantities of DOC specifically derived from  
347 permafrost and aged soils, yet the proportion of permafrost supporting DOC mineralization  
348 declines as waters move downstream through the fluvial network (Mann et al., 2015). Thus, our  
349 results importantly show that microbial metabolism continues at similar rates independent of  
350 dominant DOM source and radiocarbon age.

351           There may be several reasons for why microbial metabolism maintains this consistent  
352 rate along the flow-path, including the possibility that aquatic microorganisms are acclimating to  
353 a downstream shift in DOM composition. The higher overall amounts of bioavailable DOC we  
354 measured in soil pore waters may reflect a highly bioreactive permafrost or aged surface soil  
355 derived fraction of the bulk DOC pool (e.g., Vonk et al., 2013; Mann et al., 2014). Further  
356 downstream in larger tributary and Kolyma mainstem waters, it has been shown that lower total  
357 amounts of bioavailable DOC is supported almost entirely from predominantly modern  
358 radiocarbon aged surface soils and vegetation sources (Mann et al., 2015). Aquatic  
359 microorganisms may therefore be readily acclimating to significant shifts in DOM composition  
360 caused by selective losses of unique DOM fractions (e.g., Kaplan and Bott, 1983; Spencer et al.,  
361 2015) alongside high-internal demand for labile DOM by stream communities in lower order  
362 streams, which would otherwise generally be expected to result in decreased DOM lability with  
363 increasing water residence time (Stepanauskas et al., 1999a,b; Wikner et al., 1999; Langenheder  
364 et al., 2003; Sondergaard et al., 2003; Fellman, 2010; Fellman et al., 2014).

365           Additional mechanisms such as increasing photodegradation downstream may also  
366 account for our observed patterns in downstream DOM. Previous studies have indicated that  
367 CDOM spectral slopes (particularly  $S_{290-350}$  and  $S_{275-295}$ ) can serve as indicators of DOM source  
368 and composition, where a steeper spectral slope typically suggests lower molecular weight  
369 material with decreasing aromatic content and a shallower (i.e., lower) slope typically suggests  
370 higher molecular weight material with increasing aromatic content (Green and Blough, 1994;  
371 Blough and Del Vecchio, 2002; Helms et al., 2008; Spencer et al., 2008; Spencer et al., 2009a).  
372 Furthermore,  $S_{275-295}$  has been identified as a reliable proxy for dissolved lignin and therefore  
373 terrigenous DOM supply across Arctic Ocean coastal waters, as well as photobleaching history



374 (Helms et al., 2008; Fichot et al., 2013). We found a general increase in  $S_{290-350}$  and  $S_{275-295}$   
375 moving downstream through the network, indicative of progressive photodegradation of DOM  
376 alongside likely reductions in average DOM molecular weight and aromaticity. We found  
377 spectral slopes over longer wavelength regions ( $S_{350-400}$ ) decreased through the network, also  
378 suggesting constant photochemical degradation of DOM as waters flowed downstream (e.g.,  
379 Helms et al., 2008). The slope ratio ( $S_R$ ) has also been shown to be a proxy for DOM molecular  
380 weight and source, where low ratios typically correspond to more allochthonous, higher  
381 molecular weight DOM (Helms et al., 2008; Spencer et al., 2009b; Mann et al., 2012). The  
382 advantage of  $S_R$  ratios over individual  $S$  values is apparent when each spectral slope responds to  
383 a process in an opposing manner, emphasizing the response in calculated  $S_R$  values. The clear  
384 increases in  $S_R$  we observed moving downstream in the fluvial network (from a minimum of 0.74  
385 in soil pore waters to a maximum of 1.24 in the mainstem) indicate that during July summer  
386 conditions, soil pore waters contain higher molecular weight, aromatic terrestrial DOM that  
387 generally becomes lower in average molecular weight and aromaticity along the flow-path  
388 continuum towards the Kolyma River mainstem. The maximum  $S_R$  value of 1.24 we report in  
389 the Kolyma River mainstem is markedly higher than the range of  $S_R$  (0.82–0.92) reported in  
390 Stedmon et al. (2011) for the Kolyma from 2004 and 2005, demonstrating the heterogeneity of  
391 DOM properties even in mainstem waters and the necessity for greater temporal resolution in  
392 monitoring. Similar to spectral slopes,  $S_R$  values may also be indicative of photobleaching  
393 history (e.g., Helms et al., 2008) and our we observed increase in  $S_R$  downstream through the  
394 network suggests evidence of on-going photochemical degradation of surface water DOM during  
395 transit.

396           Photodegradation may indeed play an important and direct role in our observed consistent  
397 fraction of bioavailable DOC along the flow-path. Previous studies in the Arctic underscore the  
398 importance of residence times as well as a significant combined role for photo- and biological  
399 degradation along the flow-path in Arctic watersheds (Cory et al., 2007; Merck et al., 2012; Cory  
400 et al., 2013; Laurion and Mladenov, 2013). These previous results show that the photochemical  
401 “pretreatment” of stream DOM that occurs during export into lakes and coastal zones may  
402 impact the ability of microorganisms to mineralize DOM. Therefore, the residence times and  
403 flow-paths of waters should greatly influence the ultimate fate of DOM (e.g., DOM vs. CO<sub>2</sub>)  
404 exported to the adjacent ocean. In our case, we find that our increasing  $S_R$  values downstream  
405 suggest important photodegradation processes are occurring along the flow-path continuum,  
406 where this photodegradation may potentially release significant quantities of labile DOM for  
407 continued microbial processing of DOM further downstream in these stream networks. In other  
408 words, the more abundant “virgin” bioavailable molecules upstream are replaced downstream by  
409 photobleached smaller molecules (originating from aromatic compounds), resulting in the  
410 fraction of DOC used relatively constant without any clear pattern overall. If this (or something  
411 similar) were not the case, we would expect to see a declining fraction of bioavailable DOC  
412 along the flow-path continuum.

413           In this study, we have provided new and important findings with regards to the spatial  
414 distribution of DOM concentration, bioavailability, and optical properties during mid-summer  
415 hydrologic conditions throughout the Kolyma River basin in Northeast Siberia. Freshwater DOC  
416 measurements across the network were strongly positively correlated to CDOM absorption at  
417 254 nm ( $r^2 = 0.958$ ,  $p < 0.01$ ), confirming the utility of simple CDOM optical measurements for  
418 estimating carbon concentrations in arctic freshwaters (Spencer et al., 2008, 2009a; Stedmon et

419 al., 2011) and across water types within the Kolyma River basin in particular. Furthermore, the  
420 optical parameter  $S_R$  proved to be the only CDOM compositional measure that showed  
421 statistically significant separation between all four water types examined during the study period,  
422 suggesting that this parameter may be useful for easily distinguishing characteristics and  
423 processes occurring in organic matter among water types along the full flow-path continuum.  
424 The significant increase in  $S_R$  values we observed downstream through the network suggests  
425 evidence of on-going photochemical degradation of surface water DOM during transit.  
426 Additionally, of all the CDOM parameters,  $S_R$  values were most closely related to concentrations  
427 of bioavailable DOC ( $r^2 = 0.454$ ,  $p < 0.01$ ), suggesting that this value may be correlated with a  
428 decline in bioavailable DOC through the network. However, biological degradation has  
429 previously been shown to typically slightly decrease  $S_R$  values (Helms et al., 2008), which  
430 indicates that the opposite relationship observed here may instead be a consequence of co-  
431 variance with photodegradation of DOM, or demonstrate that  $S_R$  values may reflect a broader,  
432 more complex range of physical and biological processes than previously recognized. Garnering  
433 further insight from our measurements, the relatively constant proportion of DOC that was  
434 bioavailable regardless of relative water residence time along the flow-path may be a  
435 consequence of two potential scenarios allowing for continual processing of organic material  
436 within the system, namely: (a) aquatic microorganisms are acclimating to a downstream shift in  
437 DOM composition; and/or (b) photodegradation is continually generating labile DOM for  
438 continued microbial processing of DOM along the flow-path continuum. Without such  
439 processes, we would otherwise expect to see a declining fraction of bioavailable DOC  
440 downstream with increasing residence time of water in the system.

441 Unlike many previous studies that focus on only mainstem rivers in the Arctic, we focus  
442 here on a variety of waters along a full flow-path continuum, showing that CDOM metrics (in  
443 particular,  $S_R$ ) reflect important compositional differences in DOM of waters along the transit  
444 from headwaters to the Arctic Ocean. The range in DOM properties of waters travelling  
445 downstream through the Kolyma Basin often spanned wider ranges than DOM compositional  
446 differences reported annually among the six major arctic rivers. For example,  $S_R$  values across  
447 the major arctic rivers over the years 2004 and 2005 spanned a minimum of 0.79 in the Yenisey  
448 River, to a maximum value of 1.11 in the Mackenzie River (Stedmon et al., 2011), compared to  
449 the range of 0.74–1.24 for waters in our study within a single basin. It is therefore essential that  
450 changes taking place in the quality of CDOM exported by these rivers be examined throughout  
451 entire river basins in order to adequately assess climate driven shifts in terrigenous carbon supply  
452 and reactivity. Future work that includes both photo- and microbial degradation experiments  
453 may further elucidate the ability for  $S_R$  to serve as a direct proxy for these processes along a  
454 flow-path gradient. Our overall results thus far demonstrate promise for utilizing ultraviolet-  
455 visible absorption characteristics to easily, inexpensively, and comprehensively monitor the  
456 quantity and quality of DOM (over broad ranges) across permafrost landscapes in the Arctic.  
457 This is particularly critical for remote arctic landscapes such as those in Northeast Siberia, where  
458 the future fate of organic carbon currently frozen in permafrost soils (and whether it ultimately is  
459 released as  $\text{CO}_2$  and  $\text{CH}_4$ ) is tightly linked to the lability of this material.

460

## 461 **Acknowledgements**

462 This research was part of the Polaris Project ([www.thepolarisproject.org](http://www.thepolarisproject.org)), supported  
463 through grants from the National Science Foundation Arctic Sciences Division (Grants ARC-

464 1044560 and DUE-0732586 to K. Frey and Grants ARC-1044610 and DUE-0732944 to R.  
465 Holmes). We thank E. Bulygina, A. Bunn, B. Denfeld, S. Davydov, A. Davydova, M. Hough, J.  
466 Schade, E. Seybold, N. Zimov, and S. Zimov for assistance with field sampling collections  
467 and/or overall project coordination. We additionally thank Isabelle Laurion and two anonymous  
468 reviewers for their constructive comments and suggestions on an earlier version of this  
469 manuscript.

470

471

472

473

474

475

476

477

478

479

480

481

482

483

484

485

486

487 **References Cited**

488

489 Battin, T. J., Kaplan, L. A., Findlay, S., Hopkinson, C. S., Marti, E., Packman, A. I., Newbold, J.  
490 D., and Sabater, F.: Biophysical controls on organic carbon fluxes in fluvial networks, *Nature*  
491 *Geoscience*, 1, 95–100, 2009a.

492

493 Battin, T. J., Luysaert, S., Kaplan, L. A., Aufdenkampe, A. K., Richter, A., and Tranvik, L. J.:  
494 The boundless carbon cycle, *Nature Geoscience*, 2, 598–600, 2009b.

495

496 Blough, N. V. and Del Vecchio, R.: Chromophoric DOM in the coastal environment, in  
497 *Biogeochemistry of Marine Dissolved Organic Matter*, edited by D. A. Hansell and C. A.  
498 Carlson, pp. 509–546, Elsevier, San Diego, California, 2002.

499

500 Bronk D. A.: Dynamics of DON, in: *Biogeochemistry of Marine Dissolved Organic*  
501 *Matter*, edited by: Hansell, D. A. and Carlson, C. A., Academic Press, San Diego, pp. 153–249,  
502 2002.

503

504 Chin, Y. P., Traina, S. J., Swank, C. R., and Backhus, D.: Abundance and properties of dissolved  
505 organic matter in pore waters of a freshwater wetland, *Limnology and Oceanography*, 43(6),  
506 1287–1296, 1998.

507

508 Cole, J. J., Prairie, Y. T., Caraco, N. F., McDowell, W. H., Tranvik, L. J., Striegl, R. G., Duarte,  
509 C. M., Kortelainen, P., Downing, J. A., Middelburg, J. J., and Melack, J.: Plumbing the global  
510 carbon cycle: Integrating Inland Waters into the Terrestrial Carbon Budget. *Ecosystems*, 10,  
511 171–184, 2007.

512

513 Cory, R. M., Crump, B. C., Dobkowski, J. A., and Kling, G. W.: Surface exposure to sunlight  
514 stimulates CO<sub>2</sub> release from permafrost soil carbon in the Arctic, *Proceedings of the National*  
515 *Academy of Sciences*, 110(9), 3429–3434, 2013.

516

517 Cory, R. M., McKnight, D. M., Chin, Y.-P., Miller, P., and Jaros, C. L.: Chemical characteristics  
518 of fulvic acids from Arctic surface waters: Microbial contributions and photochemical  
519 transformations, *J. Geophys. Res.*, 112, G04S51, doi:10.1029/2006JG000343, 2007.

520

521 Cory, R. M., Ward, C. P., Crump, B. C. and Kling, G. W.: Sunlight controls water column  
522 processing of carbon in arctic fresh waters, *Science*, 345(6199), 925–928,  
523 doi:10.1126/science.1253119, 2014.

524 Denfeld, B. A., Frey, K. E., Sobczak, W. V., Mann, P. J., and Holmes, R. M.: Summer CO<sub>2</sub>  
525 evasion from streams and rivers in the Kolyma River basin, north-east Siberia, *Polar Research*,  
526 32, 19704, <http://dx.doi.org/10.3402/polar.v32i0.19704>, 2013.

527

528 Fellman, J. B., Spencer, R. G. M., Hernes, P. J., Edwards, R. T., D'Amore, D. V., and Hood, E.:  
529 The impact of glacier runoff on the biodegradability and biochemical composition of terrigenous  
530 dissolved organic matter in near-shore marine ecosystems, *Marine Chemistry*, 121, 112–122,  
531 2010.

532  
533 Fellman, J. B., Spencer, R. G. M., Raymond, P. A., Pettit, N. E., Skrzypek, G., Hernes, P. J., and  
534 Grierson, P. F.: Dissolved organic carbon biolability decreases along with its modernization in  
535 fluvial networks in an ancient landscape, *Ecology*, 95(9), 2622–2632, 2014.

536  
537 Fichot, C. G., Kaiser, K., Hooker, S. B., Zmon, R. M. W., Babin, M., Belanger, S., Walker, S.  
538 A., and Benner, R.: Pan-Arctic distributions of continental runoff in the Arctic Ocean, *Scientific*  
539 *Reports*, 3, doi:10.1038/srep01053, 2013.

540  
541 Frey, K. E. and McClelland, J. W.: Impacts of permafrost degradation on arctic river  
542 biogeochemistry, *Hydrological Processes*, 23, 169–182, 2009.

543  
544 Frey, K. E., Siegel, D. I., and Smith, L. C.: Geochemistry of West Siberian streams and their  
545 potential response to permafrost degradation, *Water Resources Research*, 43, W03406,  
546 doi:10.1029/2006WR004902, 2007.

547  
548 Frey, K. E. and Smith, L. C.: Amplified carbon release from vast West Siberian peatlands by  
549 2100, *Geophysical Research Letters*, 32, L09401, doi:10.1029/2004GL022025, 2005.

550  
551 Green, S. A., and Blough, N. V.: Optical absorption and fluorescence properties of chromophoric  
552 dissolved organic matter in natural waters, *Limnology and Oceanography*, 39, 1903–1916, 1994.

553  
554 Hayes, D. J., Kicklighter, D. W., McGuire, A. D., Chen, M., Zhuang, Q. L., Yuan, F. M.,  
555 Melillo, J. M., and Wullschlegel, S. D.: The impacts of recent permafrost thaw on land-  
556 atmosphere greenhouse gas exchange, *Environmental Research Letters*, 9(4), doi: 10.1088/1748-  
557 9326/9/4/045005, 2014.

558  
559 Helms, J. R., Stubbins, A., Ritchie, J. D., Minor, E. C., Kieber, D. J., and Mopper, K.:  
560 Absorption spectral slopes and slope ratios as indicators of molecular weight, source, and  
561 photobleaching of chromophoric dissolved organic matter, *Limnol. Oceanogr*, 53, 955–969,  
562 2008.

563  
564 Hernes, P. J., Spencer, R. G. M., Dyda, R. Y., Pellerin, B. A., Bachand, P. A. M., and  
565 Bergamaschi, B. A.: The role of hydrologic regimes on dissolved organic carbon composition in  
566 an agricultural watershed, *Geochimica et Cosmochimica Acta*, 72, 5266–5277, 2008.

567  
568 Holmes, R. M., McClelland, J. W., Peterson, B. J., Tank, S. E., Bulygina, E., Eglinton, T. I.,  
569 Gordeev, V. V., Gurtovaya, T. Y., Raymond, P. A., Repeta, D. J., Staples, R., Striegl, R. G.,  
570 Zhulidov, A. V., and Zimov, S. A.: Seasonal and annual fluxes of nutrients and organic matter  
571 from large rivers to the Arctic Ocean and surrounding seas, *Estuaries and Coasts*, 35, 369–382,  
572 doi:10.1007/s12237-011-9386-6, 2012.

573  
574 Holmes, R. M., Coe, M. T., Fiske, G. J., Gurtovaya, T., McClelland, J. W., Shiklomanov, A. I.,  
575 Spencer, R. G. M., Tank, S. E., and Zhulidov, A. V.: Climate change impacts on the hydrology  
576 and biogeochemistry of Arctic Rivers, in *Global Impacts of Climate Change on Inland Waters*,  
577 edited by C. R. Goldman, M. Kumagai, and R. D. Robarts, Wiley, 2013.

578  
579 Holmes, R. M., McClelland, J. W., Raymond, P. A., Frazer, B. B., Peterson, B. J., and Stieglitz,  
580 M.: Lability of DOC transported by Alaskan rivers to the Arctic Ocean, *Geophysical Research*  
581 *Letters*, 35, L03402, doi:10.10289/2007GL032837, 2008.  
582  
583 Judd, K. E. and Kling, G. W.: Production and export of dissolved C in arctic tundra mesocosms:  
584 the roles of vegetation and water flow, *Biogeochemistry*, 60, 213–234, 2002.  
585  
586 Kaplan, L. A. and Bott, T. L.: Microbial heterotrophic utilization of dissolved organic matter in a  
587 piedmont stream, *Freshwater Biology*, 13, 363–377, 1983.  
588  
589 Karl, D. M. and Björkman, K. M.: Dynamics of DOP. In: Hansell, D., Carlson, C. (Eds.),  
590 *Biogeochemistry of Marine Dissolved Organic Matter*, Academic Press, San Diego, pp. 249–  
591 366, 2002.  
592  
593 Langenheder, S., Kisand, V., Wikner, J., and Tranvik, L. J.: Salinity as a structuring factor for  
594 the composition and performance of bacterioplankton degrading riverine DOC, *FEMS*  
595 *Microbiology Ecology*, 45(2), 189–202, 2003.  
596  
597 Laurion, I. and N. Mladenov: Dissolved organic matter photolysis in Canadian arctic thaw  
598 ponds, *Environmental Research Letters*, 8, 035026, 2013.  
599  
600 Loiselle, S. A., Bracchini, L., Dattilo, A. M., Ricci, M., Tognazzi, A., Cozar, A., and Rossi, C.:  
601 Optical characterization of chromophoric dissolved organic matter using wavelength distribution  
602 of absorption spectral slopes, *Limnology and Oceanography*, 54(2), 590–597, 2009.  
603  
604 Mann, P. J., Davydova, A., Zimov, N., Spencer, R. G. M., Davydov, S., Bulygina, E., Zimov, S.,  
605 and Holmes, R. M.: Controls on the composition and lability of dissolved organic matter in  
606 Siberia’s Kolyma River basin, *Journal of Geophysical Research-Biogeosciences*, 117, G01028,  
607 doi:10.1029/2011JG001798, 2012.  
608  
609 Mann, P. J., Sobczak, W. V., LaRue, M. M., Bulygina, E., Davydova, A., Vonk, J., Schade, J.,  
610 Davydov, S., Zimov, N., Holmes, R. M., and Spencer, R. G. M.: Evidence for key enzymatic  
611 controls on metabolism of Arctic river organic matter, *Global Change Biology*, 20(4), 1089–  
612 1100, 2014.  
613  
614 Mann, P. J., Eglinton, T. I., McIntyre, C. P., Zimov, N., Davydova, A., Vonk, J. E., Holmes, R.  
615 M., and Spencer, R. G. M.: Utilization of ancient permafrost carbon in headwaters of Arctic  
616 fluvial networks, *Nature Communications*, doi:10.1038/ncomms8856, 2015.  
617  
618 McClelland, J. W., Holmes, R. M., Dunton, K. H., and Macdonald, R. W.: The Arctic Ocean  
619 Estuary, *Estuaries and Coasts*, 35(2), 353–368, 2012.  
620  
621 Merck M., Neilson, B., Cory, R., and Kling, G.: Variability of in-stream and riparian storage in a  
622 beaded arctic stream. *Hydrological Processes*, 26, 2938–2950, 2012.  
623



624 Moran, M. A. and Zepp, R. G.: Role of photoreactions in the formation of biologically labile  
625 compounds from dissolved organic matter, *Limnology and Oceanography*, 42(6), 1307–1316,  
626 1997.

627

628 Mulholland, P. J.: Dissolved organic matter concentrations and flux in streams, *Journal of the*  
629 *North American Benthological Society*, 16(1), 131–141, 1997.

630

631 Neff, J. C., Finlay, J. C., Zimov, S. A., Davydov, S. P., Carrasco, J. J., Schuur, E. A. G., and  
632 Davydova, A. I.: Seasonal changes in the age and structure of dissolved organic carbon in  
633 Siberian rivers and streams, *Geophysical Research Letters*, 33, L23401,  
634 doi:10.1029/2006GL028222, 2006.

635

636 Peuravuori, J. and Pihlaja, K.: Molecular size distribution and spectroscopic properties of aquatic  
637 humic substances, *Anal. Chim. Acta*, 337, 133–149, 1997.

638

639 Schreiner, K. M., Bianchi, T. S., and Rosenheim, B. E.: Evidence for permafrost thaw and  
640 transport from an Alaskan North Slope watershed, *Geophysical Research Letters*, 41(9), 3117–  
641 3126, 2014.

642

643 Sholkovitz, E. R.: Flocculation of dissolved organic and inorganic matter during mixing of river  
644 water and seawater, *Geochimica et Cosmochimica Acta*, 40(7), 831–845, 1976.

645

646 Sondergaard, M., Stedmon, C. A., and Borch, N. H.: Fate of terrigenous dissolved organic matter  
647 (DOM) in estuaries: Aggregation and bioavailability, *Ophelia*, 57(3), 161–176, 2003.

648

649 Spencer, R. G. M., Aiken, G. R., Butler, K. D., Dornblaser, M. M., Striegl, R. G., and Hernes, P.  
650 J.: Utilizing chromophoric dissolved organic matter measurements to derive export and reactivity  
651 of dissolved organic carbon exported to the Arctic Ocean: A case study of the Yukon River,  
652 Alaska, *Geophysical Research Letters*, 36, L06401, doi:10.1029/2008GL036831, 2009a.

653

654 Spencer, R. G. M., Aiken, G. R., Wickland, K. P., Striegl, R. G., and Hernes, P. J.: Seasonal and  
655 spatial variability in dissolved organic matter quantity and composition from the Yukon River  
656 basin, Alaska, *Global Biogeochemical Cycles*, 22, GB4002, doi:10.1029/2008GB003231, 2008.

657

658 Spencer, R. G. M., Mann, P. J., Dittmar, T., Eglinton, T. I., McIntyre, C., Holmes, R. M., Zimov,  
659 N., and Stubbins, A.: Detecting the signature of permafrost thaw in Arctic rivers, *Geophysical*  
660 *Research Letters*, 42, 1–6, doi:10.1002/(ISSN)1944-8007, 2015.

661

662 Spencer, R. G. M., Stubbins, A., Hernes, P. J., Baker, A., Mopper, K., Aufdenkampe, A. K.,  
663 Dyda, R. Y., Mwamba, V. L., Mangangu, A. M., Wabakanghanzi, J. N., and Six, J.:  
664 Photochemical degradation of dissolved organic matter and dissolved lignin phenols from the  
665 Congo River, *Journal of Geophysical Research*, 114, G03010, doi:10.1029/2009JG000968,  
666 2009b.

667

668 Stedmon, C. A., Amon, R. M. W., Rinehart, A. J., and Walker, S. A.: The supply and  
669 characteristics of colored dissolved organic matter (CDOM) in the Arctic Ocean: Pan Arctic  
670 trends and differences, *Marine Chemistry*, 124, 108–118, 2011.

671

672 Stepanauskas, R., Edling, H., and Tranvik, L. J.: Differential dissolved organic nitrogen  
673 availability and bacterial smniopeptidase activity in limnic and marine waters, *Microbial  
674 Ecology*, 38(3), 264–272, 1999a.

675

676 Stepanauskas, R., Leonardson, L., and Tranvik, L. J.: Bioavailability of wetland-derived DON to  
677 freshwater and marine bacterioplankton, *Limnology and Oceanography*, 44(6), 1477–1485,  
678 1999b.

679

680 Tesi, T., Semiletov, I., Hugelius, G., Dudarev, O., Kuhry, P., and Gustafsson, O.: Composition  
681 and fate of terrigenous organic matter along the Arctic land-ocean continuum in East Siberia:  
682 Insights from biomarkers and carbon isotopes, *Geochimica et Cosmochimica Acta*, 133, 235–  
683 256, 2014.

684

685 Vannote, R. L., Minshall, G. W., Cummins, K. W., Sedell, J. R., and Cushing, C. E.: The River  
686 Continuum Concept, *Canadian Journal of Fisheries and Aquatic Sciences*, 37, 130–137, 1980.

687

688 Vonk, J. E., Mann, P. J., Davydov, S., Davydova, A., Spencer, R. G. M., Schade, J., Sobczak, W.  
689 V., Zimov, N., Bulygina, E., Eglinton, T. I., and Holmes, R. M.: High biolability of ancient  
690 permafrost carbon upon thaw, *Geophysical Research Letters*, 40, 2689–2693, 2013.

691

692 Walter, K. M., Zimov, S. A., Chanton, J. P., Verbyla, D., and Chapin III, F. S.: Methane  
693 bubbling from Siberian thaw lakes as a positive feedback to climate warming, *Nature*, 443, 71–  
694 75, 2006.

695

696 Webster, J. R. and Meyer, J. L.: Organic matter budgets for streams: A synthesis, *Journal of the  
697 North American Benthological Society*, 16(1), 141–161, 1997.

698

699 Weishaar, J. L., Aiken, G. R., Bergamaschi, B. A., Fram, M. S., Fujii, R., and Mopper, K.:  
700 Evaluation of specific ultraviolet absorbance as an indicator of the chemical composition and  
701 reactivity of dissolved organic carbon, *Environ. Sci. Technol.*, 37, 4702–4708, 2003.

702

703 Wikner, J., Cuadros, R., and Jansson, M.: Differences in consumption of allochthonous DOC  
704 under limnic and estuarine conditions in a watershed, *Aquatic Microbial Ecology*, 17(3), 289–  
705 299, 1999.

706

707

708

709

710

711

712

713

714 **Table 1.** Mean spectral slope and other CDOM parameters for soil pore waters, streams, rivers,  
 715 and the Kolyma River mainstem.

716

	$S_{290-350}$ ( $\times 10^{-3} \text{ nm}^{-1}$ )	$S_{275-295}$ ( $\times 10^{-3} \text{ nm}^{-1}$ )	$S_{350-400}$ ( $\times 10^{-3} \text{ nm}^{-1}$ )	$a_{250}:a_{365}$	$\text{SUVA}_{254}$ ( $\text{L mg C}^{-1} \text{ m}^{-1}$ )	$S_R$
<b>Soil pore waters</b>	15.35	15.27	18.65	5.47	3.52	0.82
<b>Streams</b>	17.08	17.39	18.89	6.44	2.94	0.92
<b>Rivers</b>	17.17	17.79	18.19	6.27	2.77	0.98
<b>Kolyma Mainstem</b>	18.10	18.57	17.50	6.53	2.56	1.06

717

718

719

720

721 **Table 2.** Relationships between bioavailable DOC and each of the six CDOM metrics

722 investigated.  $S_R$  shows the highest r-squared value, with a  $p$ -value of 0.00002.

	$r^2$	$p$ -value
$S_{290-350}$	0.3560	0.00025
$S_{275-295}$	0.4497	0.00002
$S_{350-400}$	0.0443	0.23987
$a_{250}:a_{365}$	0.2645	0.00220
$\text{SUVA}_{254}$	0.1980	0.01376
$S_R$	0.4540	0.00002

723

724

725 **Figure Legends**

726

727 **Figure 1.** The northern reaches of the Kolyma River in East Siberia and the locations of the 47  
728 water samples collected throughout the region in this study (including soil pore waters, streams,  
729 rivers, and the Kolyma River mainstem).

730

731 **Figure 2.** Concentrations of (a) dissolved organic carbon (DOC), (b) bioavailable DOC, and (c)  
732 percentage of total DOC that is bioavailable for the four water sample types. The mean (hollow  
733 squares), median (horizontal lines),  $\pm 1$  standard deviation (gray boxes), and total range  
734 (whiskers) for each sample population are shown.

735

736 **Figure 3.** Chromophoric dissolved organic carbon (CDOM) absorption spectra from 200–800  
737 nm for (a) all samples; and (b) streams, rivers, and the Kolyma River mainstem only.

738

739 **Figure 4.** Relationships between DOC and CDOM absorption at 254, 350, and 440 nm for  
740 streams, rivers, and the Kolyma River mainstem.

741

742 **Figure 5.** The six presented CDOM metrics, (a)  $S_{290-350}$ , (b)  $S_{275-295}$ , (c)  $S_{350-400}$ , (d)  $a_{250}:a_{365}$ , (e)  
743  $SUVA_{254}$ , and (f)  $S_R$ , show the separation between soil pore, stream, river, and Kolyma mainstem  
744 waters. The mean (hollow squares), median (horizontal lines),  $\pm 1$  standard deviation (gray  
745 boxes), and total range (whiskers) for each sample population are shown.

746

747 **Figure 6.** The CDOM metric  $S_R$  shows a relatively strong relationship with concentrations of  
748 bioavailable DOC present in the sampled waters, with an r-squared value of 0.4540 and  $p$ -value  
749  $<0.01$ .

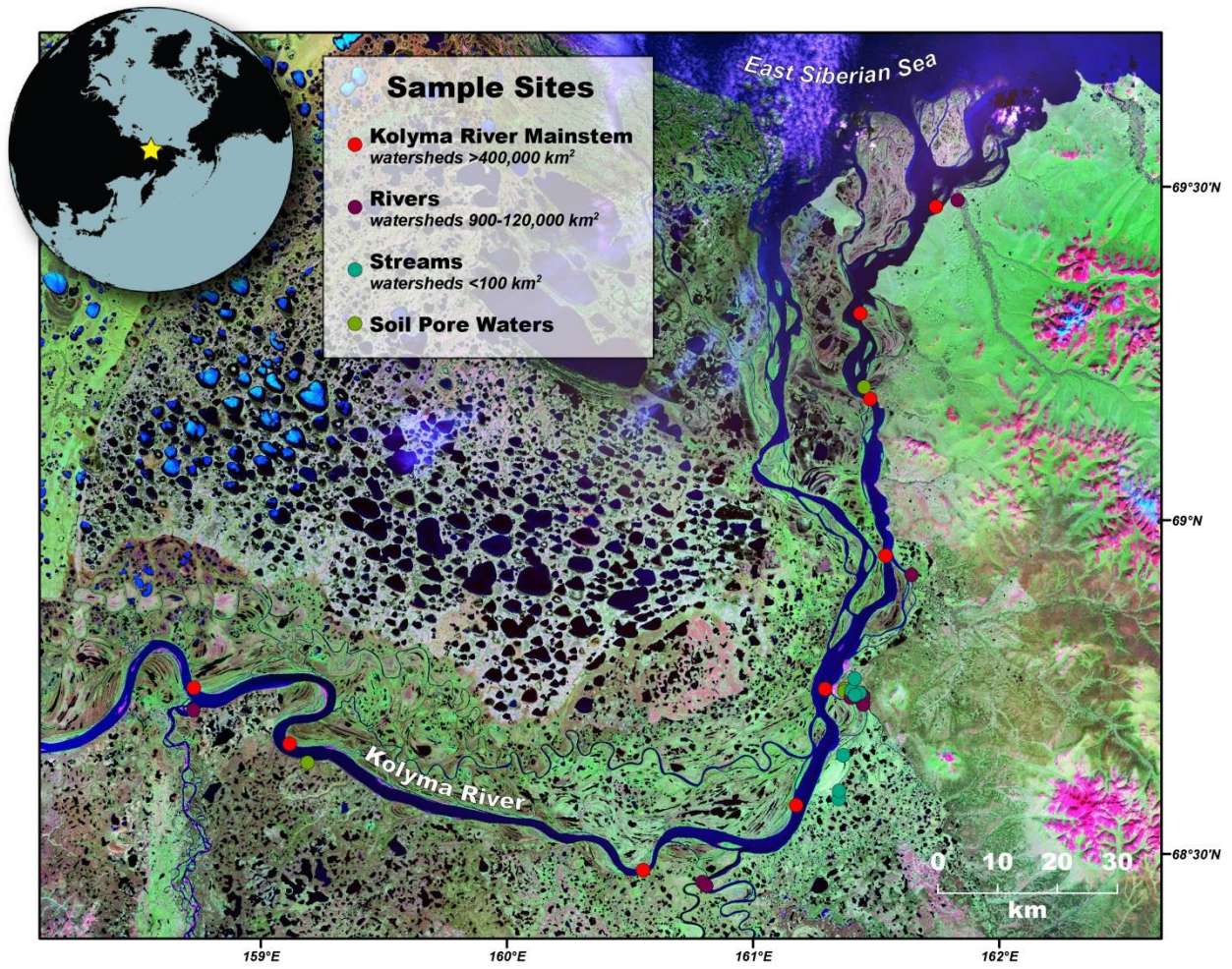


Figure 1.

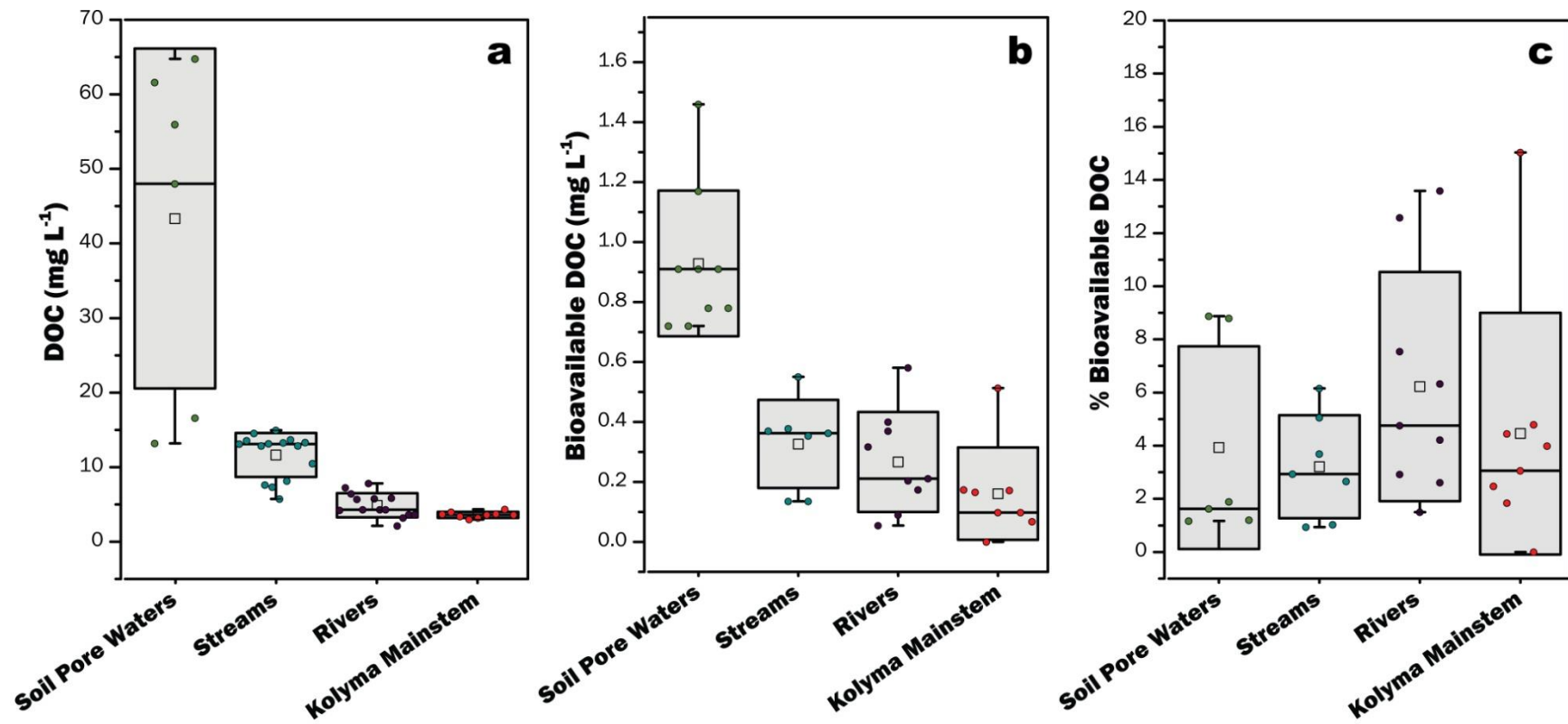


Figure 2.

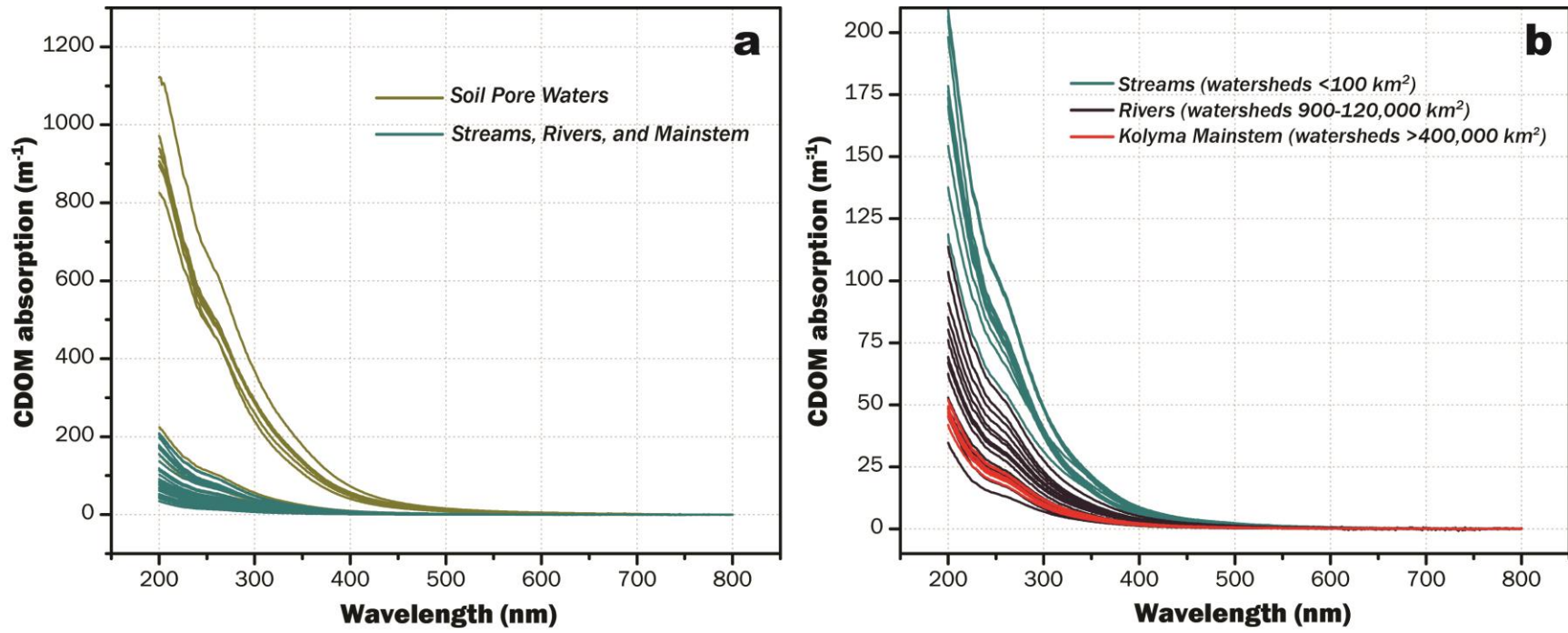


Figure 3.

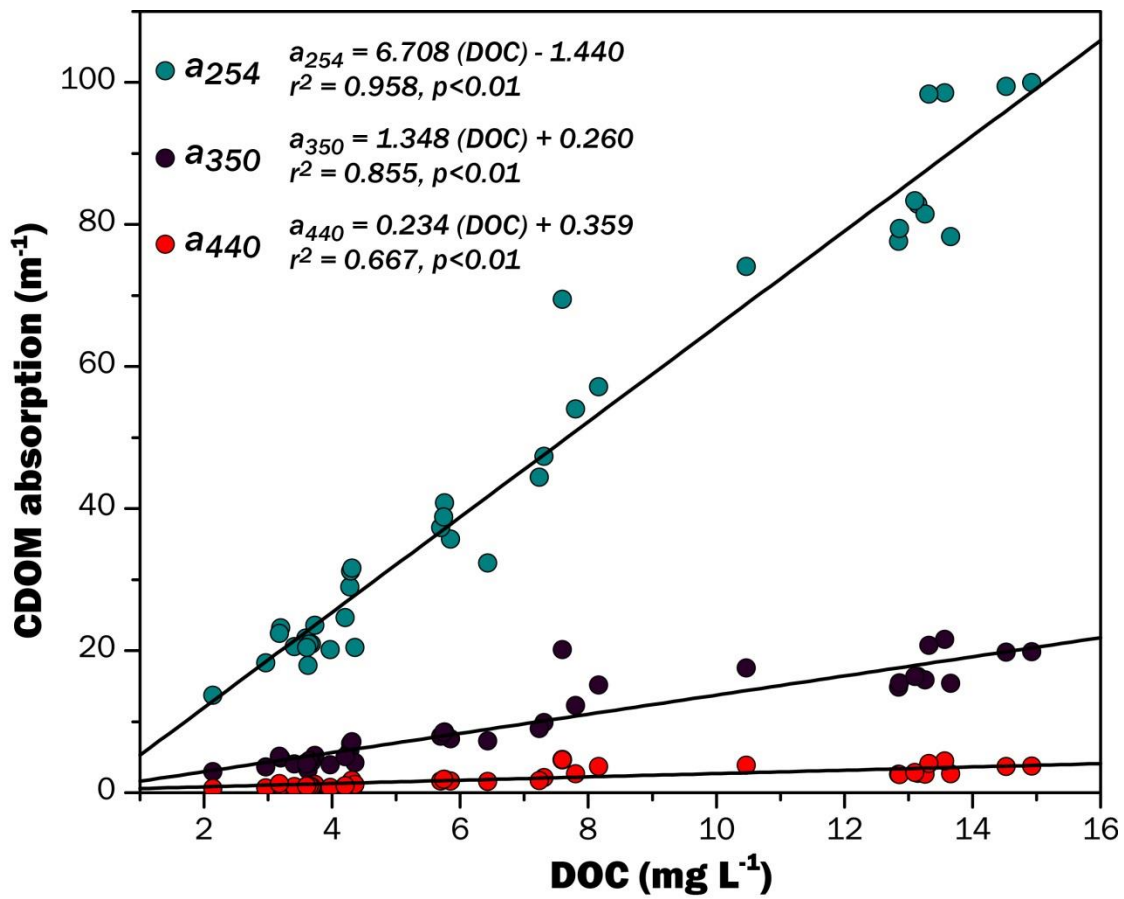


Figure 4.



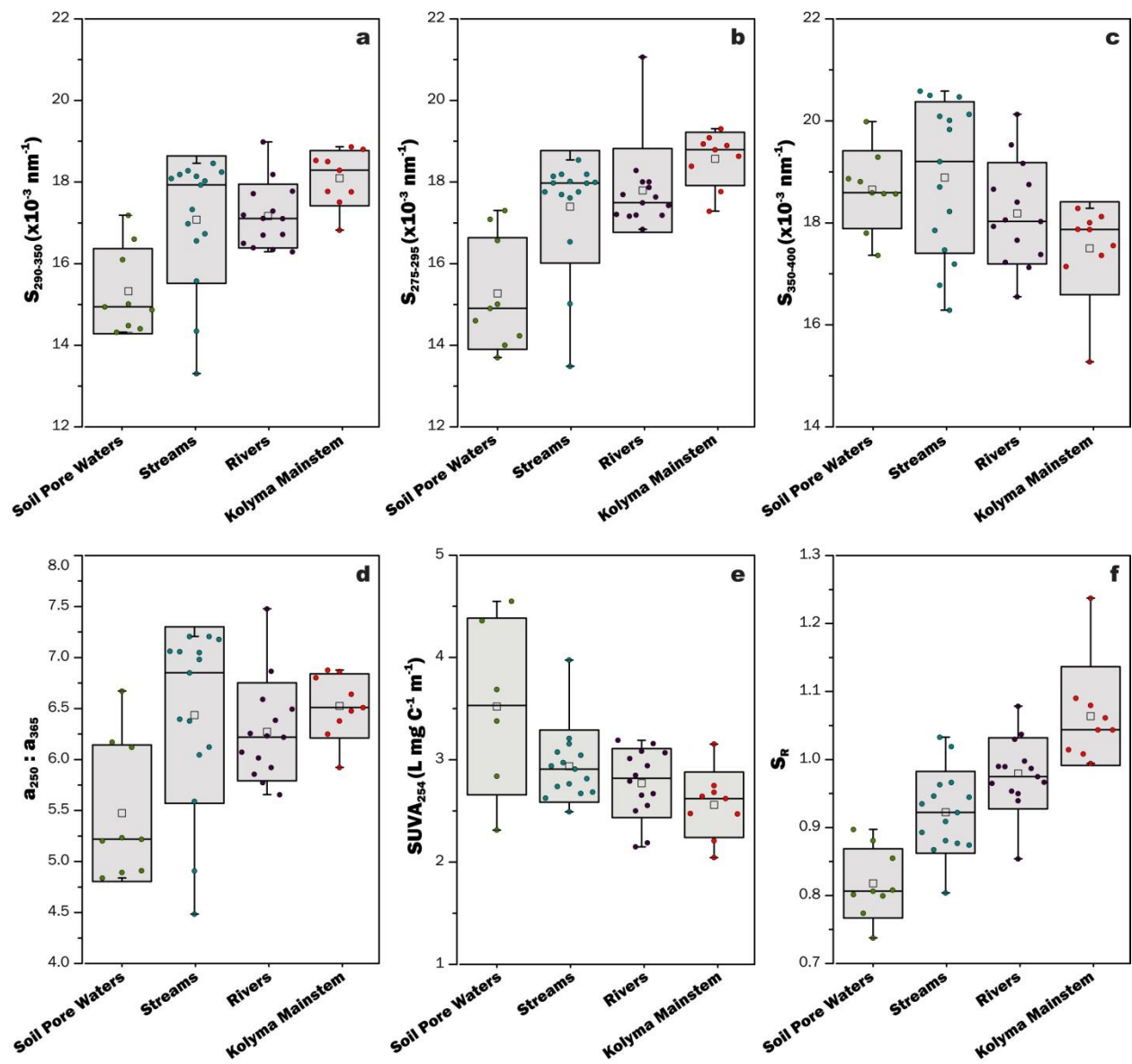


Figure 5.

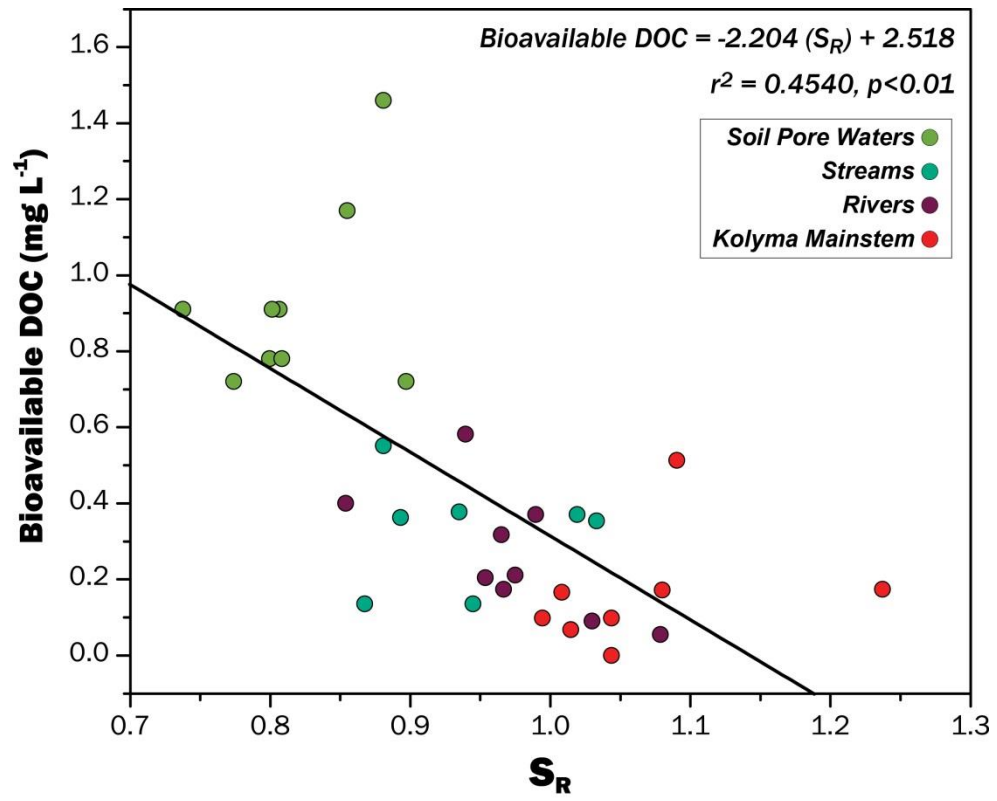


Figure 6.